Met. Mater. Int., Vol. 21, No. 1 (2015), pp. 104~108
doi: 10.1007/s12540-015-1012-x

Investigation on the Mechanism of Grain Refinement in Aluminum Alloy Solidified Under Ultrasonic Vibration

R. P. Jiang[1,2,*], X. Q. Li[1,2], and M. Zhang[1,2]

[1]Central South University, School of Mechanical and Electrical Engineering, 410083, Changsha, China
[2]Central South University, National Key Laboratory of High Performance Complex Manufacturing, 410083, Changsha, China

(received date: 21 November 2013 / accepted date: 12 April 2014)

The effect of ultrasound, chilled radiating face and dissolved Ti on the grain refinement of 7085 Al alloys was investigated in this paper. It was found that small equiaxed grains occurred below the chilled radiating face, and the coarse dendrites formed below the preheated radiating face. However, the dissolved Ti from the eroding radiator cannot generate grain refinement under ultrasonic vibration, which is different from the previously reported result that Ti is a powerful grain refiner. Significant grain refinement can be induced when the ultrasound was introduced through a preheated radiator between 650 °C and 620 °C. The grain refinement, involved in the 7085 Al alloys under ultrasonic vibration, is mainly attributed to the heterogeneous nucleation and acoustic streaming.

Keywords: alloys, casting, solidification, grain refinement, optical microscopy

1. INTRODUCTION

Generally, two different approaches, chemical inoculation and dynamic nucleation, have been widely used to achieve grain refinement during solidification [1]. The chemical inoculation depends primarily on the constitutional supercooling establishment and the nucleant selection [2], and the dynamic nucleation mainly relies on the external field, i.e. mechanical vibration, electromagnetic vibration and ultrasonic vibration [3-9]. The chemical approach brings solute pollution and/or impurities, which makes the dynamic nucleation a better option for high-purity cast alloys. The external field, like ultrasonic vibration, can induce grain refinement through altering the kinetics of nucleation and crystal growth. Grain refinement depends on the competition between nucleation and growth [2,10]. Ultrasound has attracted considerable attention in grain refinement [3-5]. A couple of mechanisms of grain refinement by ultrasound have been developed in the past few decades. The major two mechanisms are the cavitation-induced dendrite fragmentation [3,11-13] and the cavitaion-enhanced nucleation. The former proposed that the shock waves, produced by the collapse of bubbles, can result in dendrite fragmentation and, further, promote nucleation events [11]. The latter one is divided into three categories: (a) the cavitaion enhances the wettability of impurities, which enables the impurities to act as nucleation sites [14,15]; (b) the collapse of bubbles gives rise to elevated undercooling through increasing the melting point of cast metals; (c) the liquid around bubbles will be undercooled due to the bubble expansion, and then more nucleation can be initiated on the bubble surfaces [13].

Most of the mechanisms mentioned above only focus on studying the ultrasonic effect. However, some researchers have different views when discussing the role of ultrasound in grain refinement, because ultrasound was injected into the metal melts through a radiator containing Ti. In addition, the chill effect of the radiator itself can not be ignored according to the wall crystal hypothesis proposed by Ohno [16,17]. When the radiator is exposed to the liquid metal under cavitation, it will erode and introduce Ti into the melt. Therefore, Ti is also considered as an important factor in grain refinement under ultrasonic vibration. In view of these arguments, a series of experiments were designed and carried out in this paper to clarify the mechanism on the grain refinement of cast Al alloys under ultrasonic vibration.

2. EXPERIMENTAL PROCEDURE

2.1. Material and devices

Experimental material is 7085 Al alloy and the chemical compositions (wt%) are shown in Table 1. The main devices used in the experiment include a set of ultrasonic vibration system (a piezoelectric ceramic transducer, a No.45 steel amplitude transformer and a titanium alloy radiator sized

*Corresponding author: jiangripeng@163.com

Table 1. The chemical composition of 7085 Al alloy in experiment

Zn	Cu	Mg	Zr	Fe	Si	Ti	Mn	Cr	Al
7.09	1.40	1.32	0.10	0.07	0.07	0.008	0.002	0.003	Bal.

Φ50 mm×110 mm), a set of homemade digital ultrasonic generator, a resistance furnace, and two Φ180 mm× 200 mm× 18 mm graphite crucibles.

2.2. Experimental procedure

Firstly, two graphite crucibles, labeled as I and II and filled with the 7085 aluminum alloy blocks, were heated in two furnaces respectively. Then, the aluminum alloy melt was fully stirred and the oxidation layer was removed when aluminum blocks completely melted. Next, both crucible I and II were heated to 720 °C and held for fifteen minutes, then crucible I was taken out from the furnace and cooled in the air and crucible II was kept in the furnace for preheating the acoustic radiator. When the melt in crucible I cooled down to the desired temperature, the preheated ultrasonic radiator was inserted vertically 30 mm deep into the liquid (shown in Fig. 1). Meanwhile, a 20 kHz commercial ultrasonic generator was used to excite the vibration system. The amplitude attained at the radiating face is about 10 μm. Finally, the ultrasound was transformed directly into the melt from the radiating face.

The radiator was immersed 30 mm deep in the melt of crucible II for preheating. Temperature of the center point on the radiating face was monitored by an infrared radiation thermometer. The preheating was completed when the temperature tested was stable.

Five groups of experiments were designed specifically as follows:

(1) Molten alloy was solidified without ultrasonic treatment (UST).

(2) Molten alloy was solidified without UST but with a treatment of immersing a chilled radiator 30 mm deep into the liquid between 650 °C and 620 °C (the liquidus temperature of 7085 aluminum alloy was about 638 °C).

(3) Molten alloy was solidified without UST but with a treatment of immersing a preheated radiator 30 mm deep into the liquid between 650 °C and 620 °C.

(4) Molten alloy was solidified with UST through a preheated radiator being immersed 30 mm deep into the liquid between 650 °C and 620 °C.

(5) Molten alloy was solidified with UST through a preheated radiator being immersed 30 mm deep into the liquid between 680 °C and 660 °C.

Molten alloy were all solidified in the crucible and cooled in the air in the five experiments above. Besides, ultrasonic radiator was extracted from the melt immediately after the melt being processed by ultrasound or radiator in experiment (2) to (5). In the end, five ingot samples prepared were labeled as A, B, C, D and E corresponding to the five experimental conditions above. All samples were sectioned longitudinally, ground, polished and etched. Their microstructure was observed by optic microscopy. The grain size distribution was measured along the longitudinal and radial from the center of the radiating face respectively, as shown in Fig. 2. The average grain size at each position was calculated from the measurement. Besides, the average content of Ti in each ingot was detected using inductively coupled plasma-atomic emission spectrometry (ICP-AES).

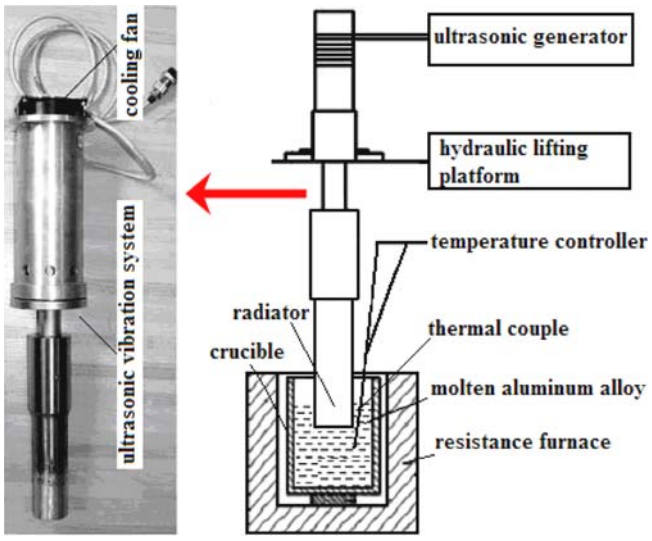

Fig. 1. Schematic diagram of ultrasonic casting experiment.

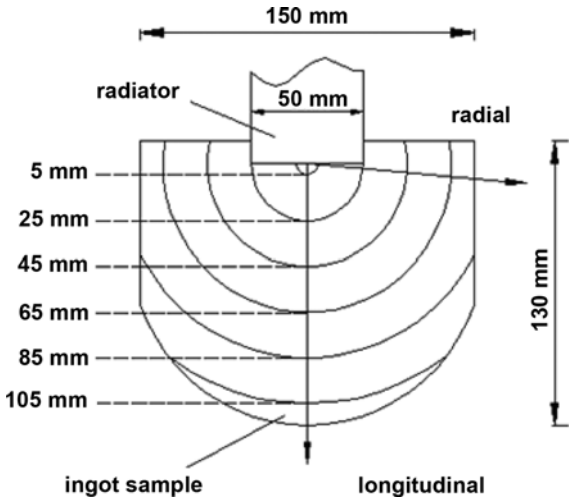

Fig. 2. Scheme of sampling in the ingot used for microstructure characterization and grain size measurement.

3. RESULTS

3.1. Microstructure characteristic

Figure 3 presents the microstructure of the selected position close to the radiating face. A coarse dendrite or columnar microstructure was found in sample A (shown in Fig. 3A) when the molten alloy was processed without any treatment. Also, similar microstructures occurred in sample C and E (shown in Fig. 3C and Fig. 3E), which indicated that grain refinement cannot be generated by either immersing a preheated radiator or applying ultrasound into the melt between 680 °C and 660 °C. The grains were refined best in sample D, grain shape of which was close to the equiaxed crystals (shown in Fig. 3D). The second was the grains of sample B where some non-dendritic a-Al crystals existed (shown in Fig. 3B).

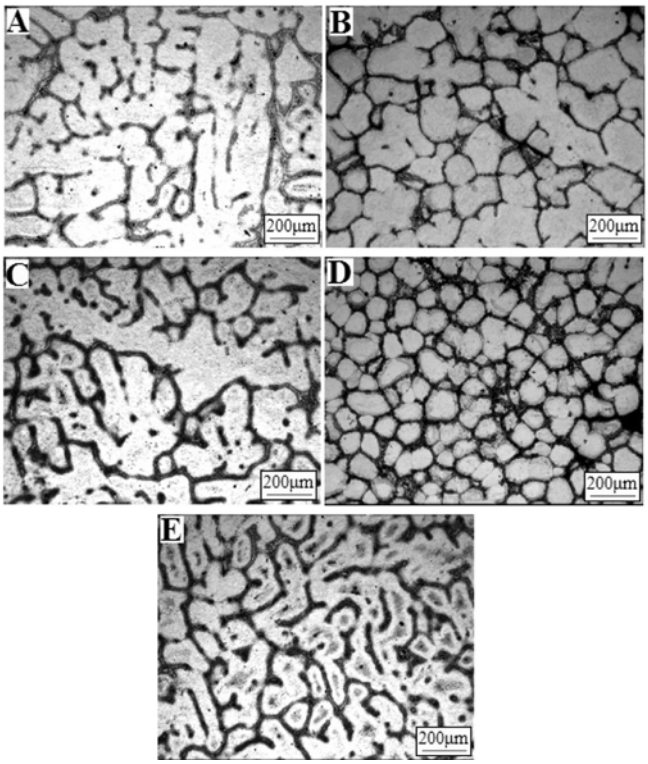

Fig. 3. Microstructures obtained under different conditions: (A) without any treatment, (B) with immersing a chilled radiator, (C) immersing a preheated radiator, (D) with UST between 650 °C and 620 °C and (E) with UST between 680 °C and 660 °C.

3.2. Grain size distribution and refinement region

From the results above, it can be known that the grains beneath the radiating face can be refined when the melt was processed either by ultrasonic vibration or by a chilled radiator. Figure 4 shows the microstructures of different locations along the longitudinal direction. It can be seen that in the condition of immersing the chilled radiator into the melt, equiaxed zone only occurred in a small area below the radiating face, and the grains are all coarse dendrite at other locations below the radiating face. Besides, microstructure became coarse with the increase of distance from the radiating. While the melt was treated by ultrasonic vibration, the non-dendritic a-Al grains were found in all areas below the radiating face and distributed homogenously.

The detailed analysis of the grain size distributions was made along the longitudinal and radial directions shown in Fig. 5. It could be seen that sizes of the grains in sample A, C and E were relatively large. Their average grain size was more than 600 μm. The grain size increases progressively with the increase of distance from the radiating face towards the crucible wall. It was worth noting that the small grains (≤300 μm) only occurred in the area 5 mm below the radiating face in sample A, but the rest of average grain size was more than 500 μm. In the samples with UST, we found that it had little influence on grain refinement by introducing ultrasound into the melt between 680 °C and 660 °C, a temperature range far from the liquidus temperature, but it can generated a significant grain refining effct between 650 °C and 620 °C. Through calculation, the average grain size of sample D was less than 250 μm.

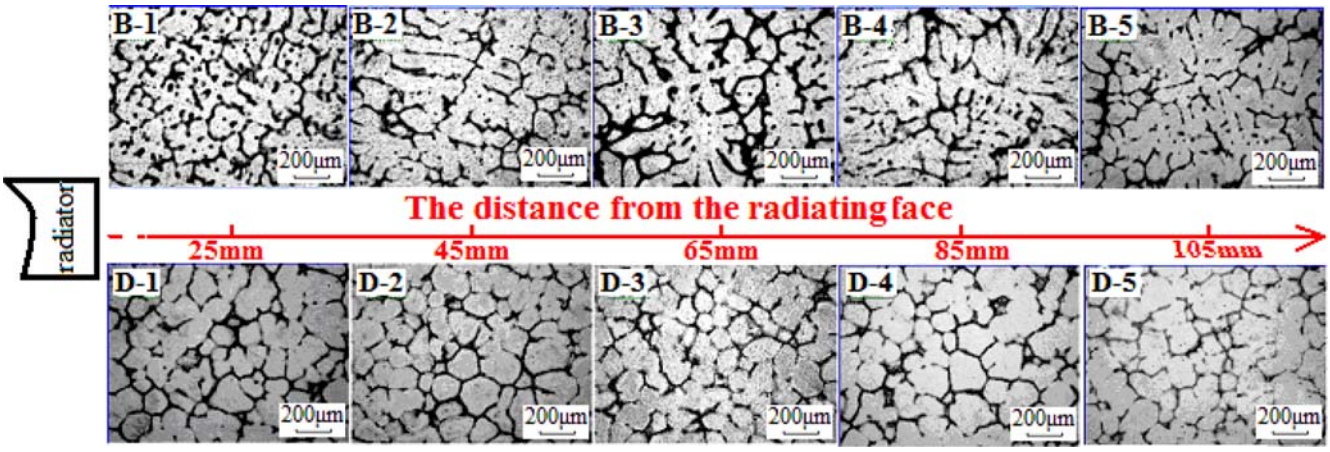

Fig. 4. Microstructures of different locations below the radiating face: (B) immersing the chilled radiator and (D) with UST.

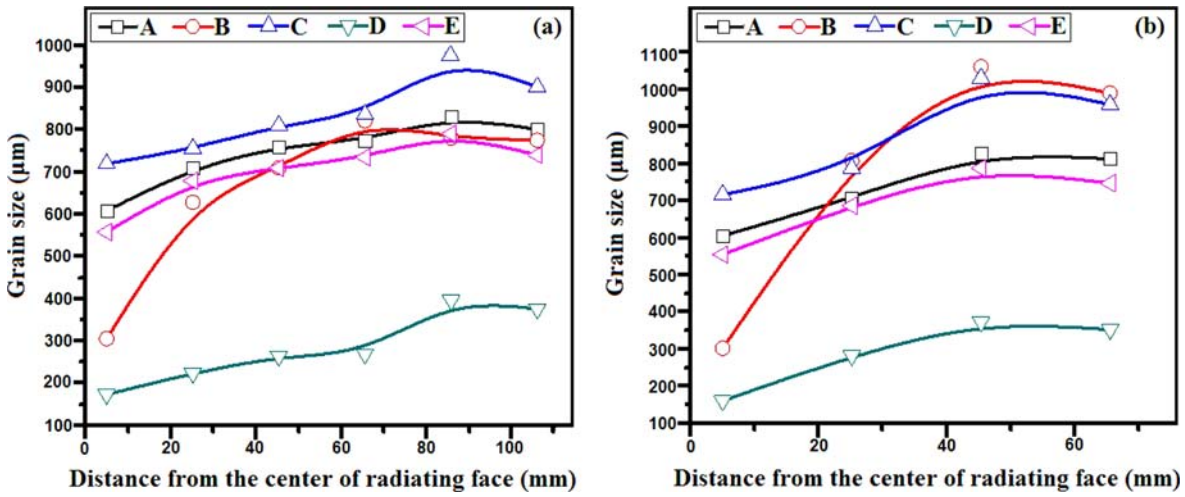

Fig. 5. Grain size distributions along (a) the longitudinal direction and (b) radial direction.

More importantly, these fine grains were distributed uniformly all over the areas below the radiating face.

4. DISCUSSION

4.1. The effect of chilled radiator on grain refinement

According to the wall crystal formation and separation hypothesis [16,17], the chilled radiator being immersed into the solidifying melt will produce nucleation on its submerged surface. Due to the gradient of solute concentration between the frontier and the foot of the newly-formed grains on mould wall, the frontier part will grow faster and gradually become a thin-neck shape. And then these wall crystals of a thin-neck shape will eventually separate from the radiating face and become the substrates of equiaxed crystals. The formation of equiaxed crystals is closely related to the temperature of mould walls. In this experiment, there is no obvious equiaxed grains below the preheated radiating face, which is mainly attributed to reduction in the undercooling after the radiator is preheated. Also because the crucible is heated with the melt in the furnaces, the microstructures close to the crucible wall are coarse. In addition, even if the chilled radiator is immersed into the melt, only a very small fine equiaxed grain zone can be formed below the radiating face. In other words, grain refinement effect induced by a chilled radiating face is quite limited.

4.2. The effect of Ti on grain refinement

As shown in Table 2, the content of Ti in samples with ultrasonic treatment was about 5 to 6 times more than the standard value. In fact, as a result of cavitaiton, the titanium alloy radiator will erode and release Ti into the melt. Al_3Ti, which is a hard brittle intermetallic compound and is easy to be broken under ultrasonic cavitation, will form during the reaction of Ti alloy and liquid aluminum [14]. It is an open question whether Al_3Ti can become heterogeneous nucleation sites. However, according to the literatures [18,19], Al_3Ti can be stable in aluminum melt if the Ti content is more than 0.15 wt%. Otherwise it will dissolve into the melts. In our experiment, the content of Ti is far less than 0.15 wt%, even, the melt was treated with ultrasonic vibration. Thus it can not become the nucleation sites. Besides, there is no grain refinement achieved in sample E, which further proves that the introduction of Ti from the eroding radiator is not the direct cause for grain refinement.

Table 2. Average content of Ti element in ingot samples

Sample	A	B	C	D	E
Ti (wt%)	0.008 (standard value)	0.009	0.010	0.039	0.046

4.3. Effect of ultrasound on grain refinement

On the mechanism of grain refinement by ultrasonic, Ohno assumed that ultrasonic vibration could promote the separation of the grains of a thin-necked shape from the mould walls. However, this theory can not adequately explain the above experimental phenomenon. It is known from the above analysis that wall grains are hard to form in the preheated radiating face and in the sidewall of crucible under ultrasonic vibration. It seems that the only source of wall crystals is the free surface [20]. However, Jiang X, Xu's study [21] has shown that ultrasonic refinement could not occur above the radiating face, which proved that free surface is not the source of wall grains. In addition, even if the formation and separation of wall grains largely contribute to the refinement under ultrasonic vibration; it is expected that the finest grain size should be observed at the bottom of the crucible below the radiating face, due to the settling of the separated wall grains. But the present work showed that the finest grain size occurred close to the radiating face at the

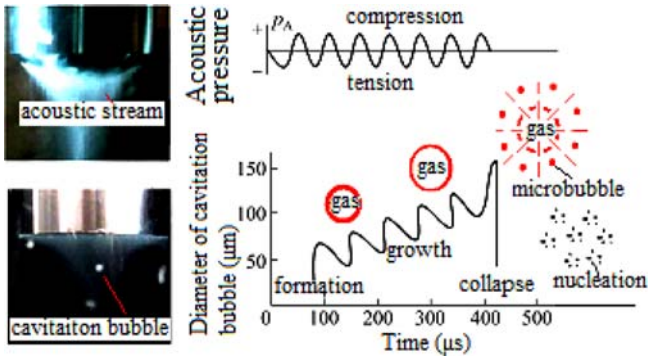

Fig. 6. Cavitation phenomenon and scheme diagram of cavitation bubble motion.

top, where the cavitaion was most severe. Therefore, the grain refinement caused by ultrasound is most likely due to the ultrasonic cavitaion.

As shown in Fig. 6, cavitation is generated by the tensile stresses of the half-period of rarefaction during the ultrasonic propagation [14]. These cavitation bubbles, with dissolved air, constantly grow up by the inertia under the compressing stress until they collapse at the breaking point and then produce the intensive shock waves [22] in metal liquid (shown in Fig. 6). The cavitation bubbles will absorb a large amount of heat from the surrounding melt as they collapse. In this way, partial undercooling occurs and the melt starts to nucleat. Also, crystal fragments broken by the shock waves further improve the nucleation events by acting as new nucleation sites. Besides, acoustic streaming can accelerate the liquid metal flow and enhance the uniformity of the melt temperature and the solute concentration, which greatly improves the nucleation environment and make grains grow up more evenly along various directions. All of these ultrasonic effects are good for the formation of fine grains. And this may explain why the fine and homogeneous grains were found in sample D. The grain size increases with distance from the radiating face, which is probably caused by the attenuation of ultrasound.

5. CONCLUSION

In summary, when the radiator is merely inserted into the melt, without imposing ultrasonic vibration, its ability on grain refinement is limited. When the melt is treated with ultrasonic vibration by a preheated radiator, the equiaxed grain microstructure occurred at all areas below the radiating face. Moreover, the nucleus of equiaxed grains produced by ultrasound are not the ones separated from the wall grains. Also, the dissolved Ti from the eroding radiator can not result in grain refinement. These experimental results support the mechanism "cavitation-promoted nucleation" for ultrasonic refinement.

ACKNOWLEDGEMENTS

This work was mainly supported by National Basic Research Program of China ('973' program) under No. 2010CB731706 and 2012CB619504 and Hunan Provincial Innovation Foundation for Postgraduate under No. CX2011B090. In addition, the authors thank for the financial support from the scholarship award for Excellent Doctoral Student granted by the Ministry of education of China.

REFERENCES

1. A. Ramirez, M. Qian, B. Davis, T. Wilks, and D. H. StJohn, *Scripta Mater.* **59**, 19 (2008).
2. D. H. StJohn, M. Qian, M. A. Easton, and P. Cao, *Acta Mater.* **59**, 4907 (2008).
3. G. I. Eskin, *Ultrason. Sonochem.* **10**, 297 (2003).
4. L. Yao, H. Hao, and S.-H. Ji, *Trans. Nonferr. Met. Soc. China*. **21**, 1241 (2011).
5. A. Das and H. R. Kotadia, *Mater. Chem. Phys*. **125**, 853 (2011).
6. F. Taghavi, H. Saghafian, and Y. H. K. Kharrazi, *Mater. Design.* **30**, 1604 (2009).
7. V. Metan, K. Eigenfeld, D. Räbiger, M. Leonhardt, and S. Eckert, *J. Alloy. Compd*. **487**, 10 (2009).
8. J. Yu, W. Ren, K. Deng, and Y. Zhong, *Acta. Metall Sin*. **22**, 35 (2009).
9. R. Haghayeghi and P.Kapranos, *Mater. Lett*. **105**, 213 (2013).
10. S. E. Offerman, N. H. van Dijk, J. Sietsma, S. Grigull, E. M. Lauridsen, L. Margulies, H. F. Poulsen, M. Th. Rekveldt, and S. van der Zwaag, *Science*. **298**, 1003 (2002).
11. H. Friedman, S. Reich, and R. Popovitz Biro, *Ultrason. Sonochem*. **20**, 432 (2013).
12. A. Das and H. R. Kotadia, *Mater. Chem. Phys*. **125**, 853 (2011).
13. K. Yasud, Y. Saiki, and T. Kubo, *Jpn. J. Appl. Phys*. **46**, 4939 (2007).
14. G. I. Eskin, *Ultrasonic Treatment of Light Alloy Melts*, p.165, Gordon & Breach, Amsterdam (1998).
15. M. Qian, A. Ramirez, and A. Das, *J. Cryst. Growth*. **14**, 3708 (2009).
16. A. Ohno, *The Solidification of Metals*, p.52, Chijin Shokan Co., Tokyo (1976).
17. A. Ohno, Solidification: *The Separation Theory and Its Practical Applications*, p.88, Springer-Verlag Berlin and Heidelberg GmbH & Co. K, Berlin (1987).
18. H. Q. Che and Q. C. Fan, *J. Alloy. Compd*. **475**, 184 (2009).
19. K. T. Kashyap and T. Chandrashekar, *Bull. Mater. Sci.* **24**, 345 (2001).
20. Y. Liu, Y. Li, and J. Guo, *J. Mater. Sci. Technol*. **19**, 376 (2003).
21. X. Jiang and H. Xu, *Mater. Lett*. **59**, 190 (2005).
22. Z. Gu, S.Wu, H. Jiang, and A. Ping, *J. Alloy. Compd*. **492**, 482 (2010).